

# Antitumor activity of MLN8054, an orally active small-molecule inhibitor of Aurora A kinase

Mark G. Manfredi\*, Jeffrey A. Ecsedy, Kristan A. Meetze, Suresh K. Balani, Olga Burenkova, Wei Chen, Katherine M. Galvin, Kara M. Hoar, Jessica J. Huck, Patrick J. LeRoy, Emily T. Ray, Todd B. Sells, Bradley Stringer, Stephen G. Stroud, Tricia J. Vos, Gabriel S. Weatherhead, Deborah R. Wysong, Mengkun Zhang, Joseph B. Bolen, and Christopher F. Claiborne

Department of Oncology, Millennium Pharmaceuticals, Inc., Cambridge, MA 02139

Edited by Joan V. Ruderman, Harvard Medical School, Boston, MA, and approved December 7, 2006 (received for review October 4, 2006)

Increased Aurora A expression occurs in a variety of human cancers and induces chromosomal abnormalities during mitosis associated with tumor initiation and progression. MLN8054 is a selective small-molecule Aurora A kinase inhibitor that has entered Phase I clinical trials for advanced solid tumors. MLN8054 inhibits recombinant Aurora A kinase activity *in vitro* and is selective for Aurora A over the family member Aurora B in cultured cells. MLN8054 treatment results in G<sub>2</sub>/M accumulation and spindle defects and inhibits proliferation in multiple cultured human tumor cell lines. Growth of human tumor xenografts in nude mice was dramatically inhibited after oral administration of MLN8054 at well tolerated doses. Moreover, the tumor growth inhibition was sustained after discontinuing MLN8054 treatment. In human tumor xenografts, MLN8054 induced mitotic accumulation and apoptosis, phenotypes consistent with inhibition of Aurora A. MLN8054 is a selective inhibitor of Aurora A kinase that robustly inhibits growth of human tumor xenografts and represents an attractive modality for therapeutic intervention of human cancers.

cancer | mitosis | apoptosis

Aurora A and Aurora B are structurally related serine/threonine protein kinases that function during mitosis. In humans, these enzymes share 75% sequence homology in their kinase domains (1, 2). Despite similarities in name and structure, Aurora A and Aurora B carry out distinct activities in mitosis. Aurora A is expressed early in mitosis and localizes to centrosomes and proximal mitotic spindles (3). Aurora A phosphorylates a variety of proteins, including TPX2, TACC3, Eg5, and p53, among others (4). Inactivating mutations in Aurora A or targeted protein depletion in cells derived from *Drosophila melanogaster*, *Xenopus laevis*, *Caenorhabditis elegans*, and human tumors prevent centrosome maturation, resulting in improper formation of the mitotic spindle (5–9). In addition, disruption of Aurora A protein in tumor cells delays mitotic entry and progression, resulting in the accumulation of cells in the G<sub>2</sub>/M cell cycle phase (9–13). Aurora B localizes to kinetochores in mitosis and to the midbody during cytokinesis (3), where it phosphorylates several proteins, including INCENP (inner centromere protein), Histone H3, and RacGAP, among others (4, 14). Inhibition of Aurora B in mammalian cells prevents proper alignment of chromosomes to the spindle plate, inhibits cytokinesis, and results in the formation of multinucleated cells (15–18).

The Aurora A gene is amplified and overexpressed in cancers originating from multiple tissue types (19). Increased Aurora A expression may lead to increased kinase activity, which is thought to contribute to tumor initiation and progression (20). This suspected oncogenic role of Aurora A, in addition to its essential role in mitotic progression, make it an attractive target for anticancer therapy. Small-molecule inhibitors of human Aurora kinases have been identified by several groups. Although these molecules were found to inhibit both Aurora A and Aurora B protein kinases *in vitro*, the major cellular phenotypic response they produced was consistent with inhibition of Aurora B (15, 18, 21–24). It has been suggested these dual Aurora A and Aurora B inhibitors mediate antitumor activity primarily through inhibition of Aurora B activity

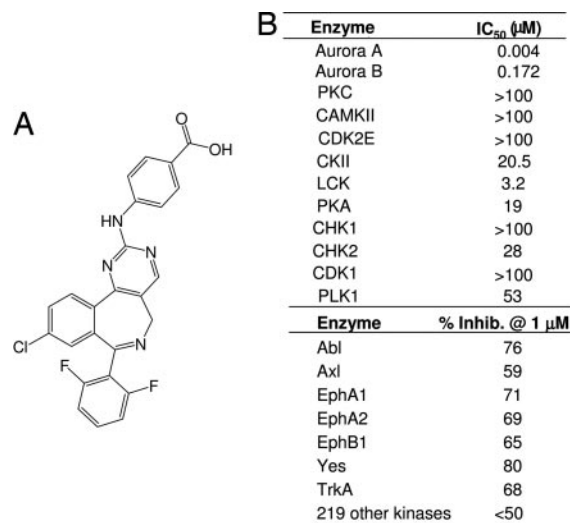


**Fig. 1.** MLN8054 is a potent and selective inhibitor of Aurora A kinase. (A) Chemical structure of 4-[[9-chloro-7-(2,6-difluorophenyl)-5H-pyrido[5,4-d][2]benzazepin-2-yl]amino]-benzoic acid. (B) IC<sub>50</sub> values of MLN8054 against recombinant Aurora A, Aurora B, and a panel of other selected kinases. Kinase activity was assessed by using radioactive FlashPlate assays as described in *Methods*. Percent inhibition for 226 kinases was determined at 1 μM MLN8054 as described in *Methods*.

(25, 26). A recent study has shown that one of these dual inhibitors also produces a phenotype consistent with Aurora A kinase inhibition, namely mitotic spindle abnormalities (27).

In this report, we describe MLN8054, an orally active small-molecule inhibitor of Aurora A kinase that has entered clinical development. MLN8054 inhibits proliferation of multiple cultured tumor cell lines and demonstrates potent oral antitumor activity in mice bearing human tumor xenografts.

Author contributions: M.G.M., J.A.E., K.A.M., S.K.B., W.C., K.M.G., B.S., J.B.B., and C.F.C. designed research; K.A.M., O.B., W.C., K.M.H., J.J.H., P.J.L., E.T.R., T.B.S., S.G.S., T.J.V., G.S.W., D.R.W., and M.Z. performed research; and M.G.M., J.A.E., and K.A.M. wrote the paper.

Conflict of interest statement: The authors of this paper, who are employees of Millennium Pharmaceuticals, Inc., are stock holders in the company.

This article is a PNAS direct submission.

Abbreviations: pHisH3, phosphorylated Histone H3; pT288, Aurora A autophosphorylation on Thr-288; TGI, tumor growth inhibition; QD, once per day; BID, twice per day.

\*To whom correspondence should be addressed at: Millennium Pharmaceuticals Inc., 40 Landsdowne Street, Cambridge, MA 02139. E-mail: manfredi@mpi.com.

This article contains supporting information online at [www.pnas.org/cgi/content/full/0608798104/DC1](http://www.pnas.org/cgi/content/full/0608798104/DC1).

© 2007 by The National Academy of Sciences of the USA

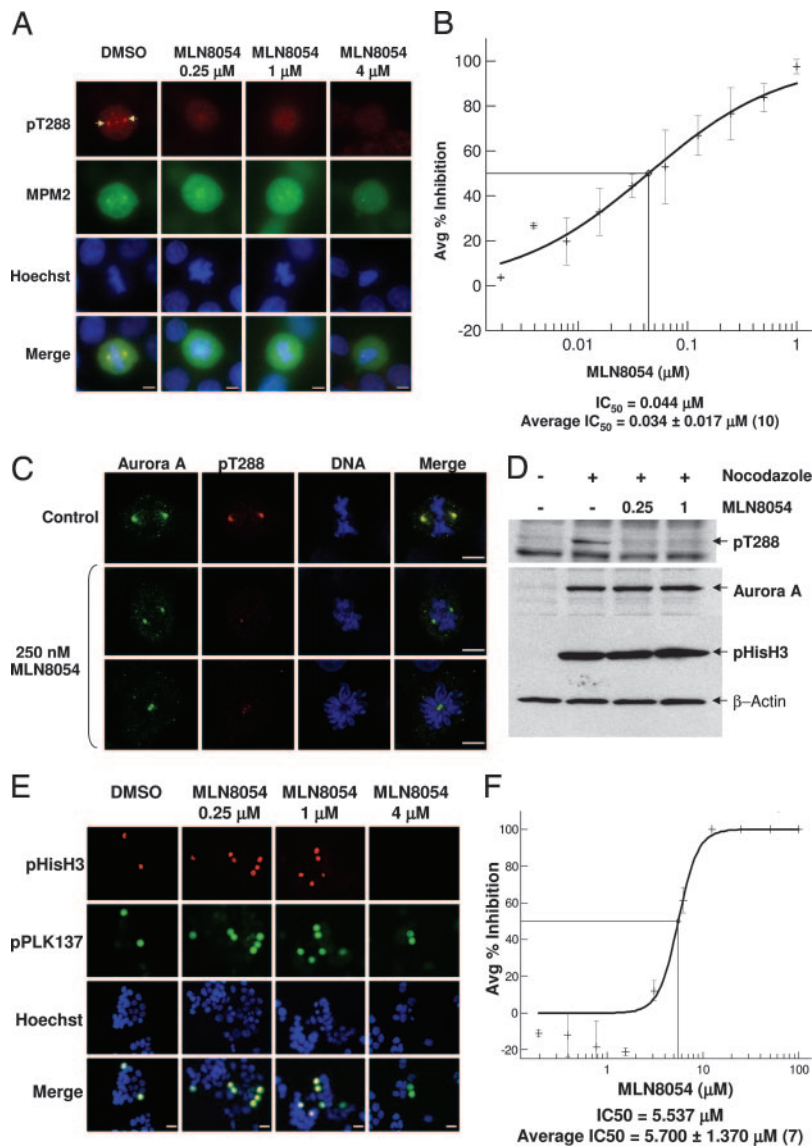


**Fig. 2.** MLN8054 selectively inhibits Aurora A over Aurora B in cultured human tumor cells. (A) Representative immunofluorescent images of HCT-116 cells treated with DMSO or MLN8054 at various concentrations for 24 h. Cells were stained for pT288 (red), MPM2 (green), and DNA (blue). Overlapping localization is shown in the merged images. Arrows indicate Aurora A autophosphorylation on Thr-288, occurring on the centrosomes. (Scale bars, 5  $\mu\text{m}$ .) (B) An Aurora A pT288 autophosphorylation assay was used to measure inhibition of Aurora A by MLN8054 in HeLa cells. The concentration–response curve was generated by calculating the decrease of Aurora A pT288 fluorescent intensity in MLN8054-treated samples relative to the DMSO-treated controls. (C) Immunofluorescent images of HCT-116 cells treated with DMSO or MLN8054 at 250 nM for 24 h. Cells were stained for Aurora A (green), pT288 (red), and DNA (blue). Overlapping localization is shown in the merged images. (Scale bars, 5  $\mu\text{m}$ .) (D) Western blots of nocodazole-arrested cells treated with various concentrations of MLN8054 probed for pT288, Aurora A, pHisH3, and  $\beta$ -actin. (E) Representative immunofluorescent images of HCT-116 cells treated with DMSO or MLN8054 at various concentrations for 24 h. Cells were stained with pHisH3 (Ser-10) mouse monoclonal antibody (pHisH3; red), phospho-PLK (Ser-137, mitotic cells) rabbit antibody (pPLK137; green), and Hoechst (blue). Overlapping localization is shown in the merged images. (Scale bars, 10  $\mu\text{m}$ .) (F) An Aurora B Ser-10 pHisH3 phosphorylation assay was used to measure the inhibition of Aurora B by MLN8054 in HeLa cells. Concentration–response curves were generated by calculating the ratio of Ser-10 pHisH3-positive cells to total mitotic cells in MLN8054-treated samples relative to the DMSO-treated controls. (B and F) For both curves, the points represent averages of three to four replicate samples  $\pm$  SD (bars). Bisecting lines reflect compound  $\text{IC}_{50}$  values. The  $\text{IC}_{50}$  number was calculated from the curves shown. Average  $\text{IC}_{50}$  numbers represent the average  $\text{IC}_{50}$  ( $\mu\text{M}$ )  $\pm$  SD derived from multiple experiments, indicated by the number in parentheses.

## Results

### MLN8054, a Potent and Selective Inhibitor of Aurora A Kinase Activity.

MLN8054 has a benzazepine core scaffold with a fused amino pyrimidine ring and an aryl carboxylic acid which, to our knowledge, represents an unprecedented kinase inhibitor framework (Fig. 1A). MLN8054 is an ATP-competitive, reversible inhibitor of recombinant Aurora A kinase [supporting information (SI) Fig. 6] with an  $\text{IC}_{50}$  value of 4 nM (Fig. 1B). MLN8054 was >40-fold more selective for Aurora A compared with the family member Aurora B and >100-fold selective for Aurora A compared with a panel of other kinases for which  $\text{IC}_{50}$  values were generated (Fig. 1B). Moreover, of 226 kinases tested at 1  $\mu\text{M}$ , only 7 had inhibitory activities of <50% (SI Fig. 7).

### MLN8054 Selectively Inhibits Aurora A Over Aurora B in Cultured Cells.

The effect of MLN8054 on Aurora A activity in HCT-116 colon tumor cells was evaluated by immunofluorescent detection of Aurora A autophosphorylation on Thr-288 (pT288) (Fig. 2A). Aurora A kinase activity depends on autophosphorylation of T288 in the activation loop (28, 29). Thus, detection of Aurora A autophosphorylation on T288 reflects the activity of the kinase in cells. In control (DMSO-treated) cells, pT288 was detected only in mitotic cells and was localized to the centrosomes. Treatment of

HCT-116 cells with MLN8054 for 24 h at 0.25, 1, and 4  $\mu\text{M}$  inhibited Aurora A autophosphorylation on T288. Total Aurora A was still present upon MLN8054 treatment, demonstrating that the decreased pT288 staining was due to inhibition of phosphorylation and not Aurora A degradation or down-regulation (Fig. 2C). The decreased Aurora A phosphorylation on pT288 was corroborated in nocodazole-arrested cells treated with MLN8054 (Fig. 2D). Although the possibility of inhibiting an upstream kinase cannot be ruled out, the data from a panel of >200 kinases (Fig. 1B and SI Fig. 7) suggest that MLN8054 is selective. A quantitative cell-based assay was developed to determine the potency of MLN8054 against Aurora A in cells by measuring the immunofluorescent intensity of pT288 in mitotic HeLa cells (Fig. 2B). In this assay, MLN8054 inhibited Aurora A in 1 h with an average  $\text{IC}_{50}$  of  $0.034 \pm 0.016 \mu\text{M}$ .

The selectivity of MLN8054 for Aurora A over the structurally related Aurora B kinase was evaluated in HCT-116 tumor cells by immunofluorescent detection of phosphorylated Histone H3 (pHisH3) on Ser-10, an Aurora B-specific substrate in cells (Fig. 2E) (30, 31). Although MLN8054 at 0.25 and 1  $\mu\text{M}$  suppressed Aurora A activity, these concentrations were not sufficient to inhibit Aurora B activity, because mitotic (pPLK137-immunopositive) cells remained pHisH3-immunopositive. However, when treated with 4  $\mu\text{M}$  MLN8054 for 24 h, no mitotic cells

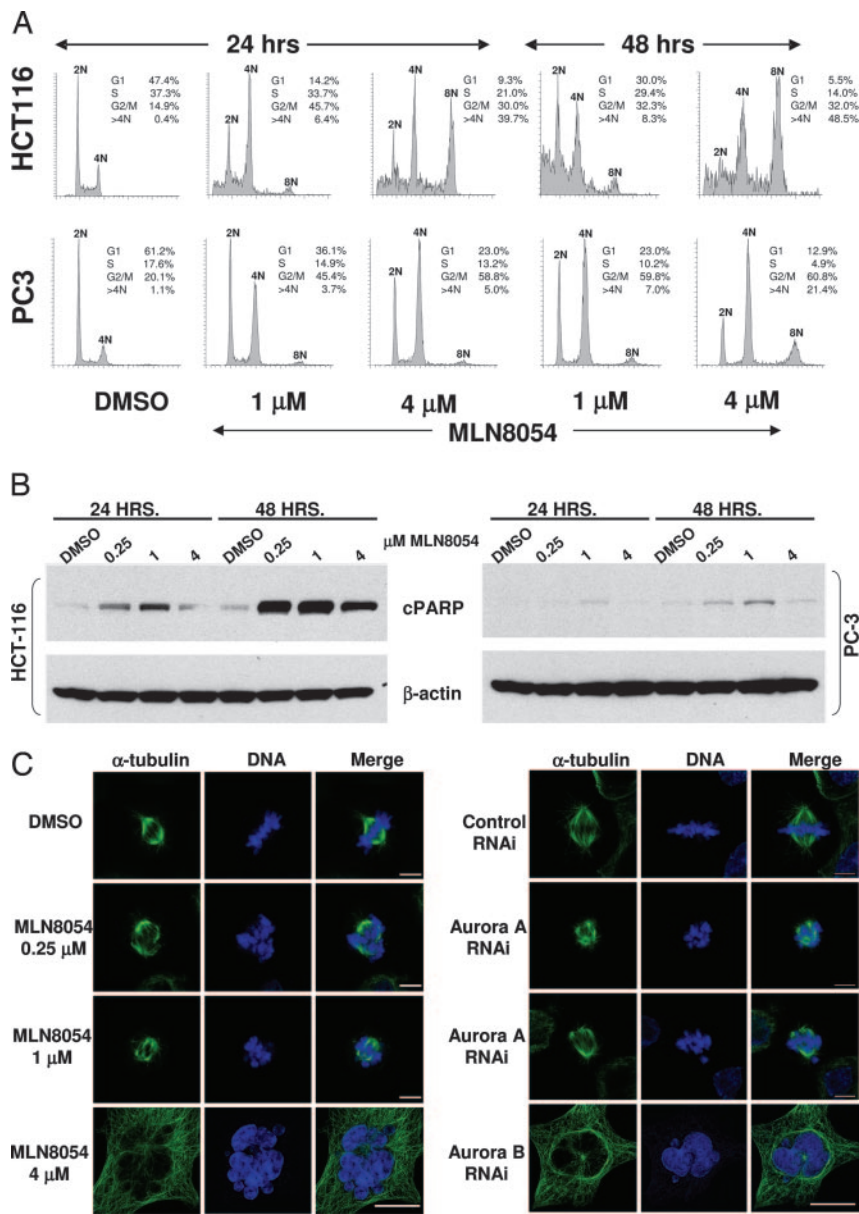


**Fig. 3.** Low and high concentrations of MLN8054 result in cellular phenotypes consistent with Aurora A and Aurora B inhibition, respectively, and induce apoptosis. (A) DNA profiles of HCT-116 and PC3 cells treated with DMSO or MLN8054 at 1 or 4  $\mu$ M for 24 or 48 h were evaluated by flow cytometry. 2N, 4N, and 8N reflect relative DNA content and represent diploid, tetraploid, and multinucleated cells, respectively. The percentage of cells in G<sub>1</sub>, S, G<sub>2</sub>/M and with >4N DNA content is shown. (B) Detection of apoptosis in HCT-116 and PC3 cells with cleaved PARP using Western blot analysis. Cells were treated with DMSO or MLN8054 at 0.25, 1, or 4  $\mu$ M for 24 or 48 h. (C) Representative immunofluorescent images of HCT-116 cells treated with DMSO or MLN8054 at 0.25, 1, and 4  $\mu$ M for 24 h or RNAi for control, Aurora A, or Aurora B. Overlapped images were obtained from cells stained with anti- $\alpha$ -tubulin mouse antibody (tubulin; green) and Hoechst (DNA; blue). (Scale bars: DMSO-treated, 0.25 and 1  $\mu$ M MLN8054-treated, and Aurora A RNAi-treated cells, 5  $\mu$ m; 4  $\mu$ M MLN8054-treated and Aurora B RNAi-treated cells, 20  $\mu$ m.)

stained positive for pHisH3, demonstrating that Aurora B activity was inhibited with higher concentrations of MLN8054. A second cell-based assay was developed to determine the potency of MLN8054 against Aurora B kinase activity by quantifying pHisH3-immunopositive mitotic cells (Fig. 2F). In this assay, MLN8054 inhibited Aurora B in 1 h with an IC<sub>50</sub> of 5.7  $\pm$  1.4  $\mu$ M. Thus, the data from the Aurora A and Aurora B cell-based assays suggest that MLN8054 has a >150-fold greater potency against Aurora A compared with Aurora B.

**MLN8054 Delays G<sub>2</sub>/M Progression in Cultured Human Tumor Cells.**

The effect of MLN8054 on the cell cycle was examined by evaluating DNA profiles using flow cytometry (Fig. 3A). In both HCT-116 colorectal and PC-3 prostate human tumor cells, treatment with 1  $\mu$ M MLN8054 for 24 and 48 h induced increased 4N cells relative to control cells. Quantification of MPM2 (mitotic marker) immunopositive HCT-116 and PC3 cells demonstrated that the percentage of mitotic cells increased from  $\approx$ 4% to 12% upon treatment with MLN8054 for 24 h at this concentrations (data not shown). The increase in mitotic cells is consistent with a delay in mitotic

progression known to occur upon Aurora A inhibition (9). However, an increase in mitotic cells to  $\approx$ 12% cannot account entirely for the dramatic increase in 4N cells shown in Fig. 3A. It is likely that, in addition to cells delayed in mitosis, the increased 4N population derives from cells delayed in G<sub>2</sub>, which is also known to occur upon Aurora A inhibition (9–12). A prominent subG<sub>1</sub> cell population can be seen at 24 and 48 h after MLN8054 treatment, which is indicative of apoptosis (Fig. 3A). These results were confirmed by an increase of cleaved PARP in treated cells (Fig. 3B).

The morphology of mitotic spindles and chromosomes were examined in HCT-116 cells treated with MLN8054. The DMSO-treated control cells displayed normal bipolar mitotic spindles with chromosomes properly aligned along the metaphase plate (Fig. 3C). MLN8054 at 0.25 and 1  $\mu$ M induced the formation of abnormal mitotic spindles, with various degrees of chromosome alignment defects. Formation of abnormal mitotic spindles is consistent with a known Aurora A inhibition phenotype (5–9), including when Aurora A is depleted by using RNAi (Fig. 3C). Aurora A plays a pivotal role in centrosome maturation and spindle formation during mitosis. Therefore, inhibition of Au-



**Table 1. Growth inhibition (IC<sub>50</sub>) across various cell lines by MLN8054**

Cell line	Origin	MLN8054, $\mu$ M
HCT-116	Colon tumor	0.18 $\pm$ 0.06 (3)
SW480	Colon tumor	0.86 $\pm$ 0.40 (2)
DLD-1	Colon tumor	1.43 (1)
MCF-7	Breast tumor	0.67 (1)
MDA-MB-231	Breast tumor	0.74 $\pm$ 0.01 (2)
Calu-6	Lung tumor	0.22 $\pm$ 0.09 (3)
H460	Lung tumor	0.11 $\pm$ 0.06 (2)
SKOV-3	Ovary tumor	0.53 (1)
PC-3	Prostate tumor	0.79 (1)

Numbers represent average IC<sub>50</sub>  $\pm$  SD derived from a BrdU cell proliferation ELISA. Values in parentheses represent the number of experiments completed for each cell line.

rorA activity with low concentrations of MLN8054 inhibits cells from progressing through mitosis normally and can result in aberrant mitotic spindle formation.

Flow cytometry and immunofluorescence also were used to analyze cells treated with a higher concentration of MLN8054 that inhibits Aurora B in addition to Aurora A. In HCT-116 cells, treatment with 4  $\mu$ M MLN8054 for 24 and 48 h resulted in a dramatic increase in 8N cells when DNA profiles were analyzed by flow cytometry (Fig. 3A). 8N cells were present at a much lower level in HCT-116 and PC3 cells treated with 1  $\mu$ M MLN8054. The 8N peak is indicative of multinucleated cells, which was corroborated by the appearance of unusually large nuclei when HCT-116 cells treated with 4  $\mu$ M MLN8054 were visualized by immunofluorescence (Fig. 3C). Multinucleation is a phenotype consistent with inhibition of Aurora B (15, 16, 27), which was confirmed by Aurora B RNAi (Fig. 3C). Aurora B provides an essential function for the spindle assembly checkpoint (15, 17, 18), which is responsible for coordinating proper attachment of the mitotic spindle apparatus to chromatin, and orchestrates mitotic events. When this checkpoint is compromised, cells can exit mitosis without undergoing cytokinesis, and enter G<sub>1</sub> with a 4N (tetraploid) DNA content (32, 33). Certain cell types are then able to undergo endoreduplication resulting in multinucleated (8N) cells. The role of Aurora B in the spindle checkpoint likely explains the dominance of the Aurora B phenotype (multinucleation) relative to the Aurora A phenotype (accumulation of mitotic cells) when cells were treated with 4  $\mu$ M MLN8054. These results are consistent with previously published data (34). Interestingly, the PC-3 cells undergo multinucleation to a lesser degree than HCT-116 after 48 h of treatment with 4  $\mu$ M MLN8054 (Fig. 3A). This result is possibly due to the slower doubling time of these cells. Collectively, the above data demonstrate that in these cultured human tumor cells, MLN8054 treatment at lower concentrations elicited phenotypes consistent with known Aurora A inhibition.

**MLN8054 Inhibits Proliferation of Cultured Human Tumor Cells and Growth of Xenografts in Nude Mice.** BrdU cell proliferation assays were used to evaluate the growth of nine cell lines treated with

MLN8054 (Table 1). MLN8054 effectively inhibited the growth of cells from diverse tissue origins with IC<sub>50</sub> values ranging from 0.11 to 1.43  $\mu$ M.

The antitumor activity of MLN8054 was evaluated by using HCT-116 and PC-3 human tumors grown as xenografts in nude mice. In the HCT-116 tumor-bearing mice, MLN8054 was administered orally at 3, 10, and 30 mg/kg once a day (QD) for a period of 21 days. Dose-dependent tumor growth inhibition (TGI) was demonstrated compared with vehicle-treated mice. TGI in the 10 and 30 mg/kg dose groups was significant compared with vehicle controls and was 76% ( $P < 0.01$ ) and 84% ( $P < 0.001$ ), respectively, after 21 days of treatment (Fig. 4A). Moreover, TGI was sustained for >1 week after treatment was stopped in the 30 mg/kg QD group. MLN8054 was well tolerated at all doses, with <2% average body weight loss in the 30 mg/kg group (at the end of treatment). Comparable efficacy was seen in HCT-116 tumor bearing mice treated with 30 mg/kg twice a day (BID) (60 mg $\cdot$ kg<sup>-1</sup> $\cdot$ day<sup>-1</sup>; TGI 96%; data not shown). MLN8054 dosed 30 mg/kg BID resulted in a decrease in body weight of 7.5% with a 73% drop in neutrophil counts. Body weight and neutrophil counts recovered after treatment stopped, suggesting that these effects were reversible.

MLN8054 also inhibited the growth of the PC-3 tumor xenograft in nude mice. In this study, MLN8054 was administered orally at 10 and 30 mg/kg BID and 30 mg/kg QD for a period of 21 days. Tumor volumes were calculated for an additional 3 weeks after MLN8054 treatment stopped to determine the durability of response. TGI in all MLN8054-treated groups was similar (73–93%) and statistically significant ( $P < 0.001$ ) compared with the vehicle controls at the end of dosing (Fig. 4B). MLN8054 doses of 30 mg/kg QD (TGI, 81%) and BID (TGI, 93%) were similarly efficacious. Remarkably, TGI was sustained after treatment was withdrawn, with the greatest tumor growth delay seen in the 30 mg/kg BID dose group, lasting for > 3 weeks after treatment had ended. Several tumors in this group did start to regrow after the 3-week period. MLN8054 was well tolerated at all doses, with the high-dose group (30 mg/kg BID) losing an average of 5.4% of initial body weight on day 21 of treatment. In both tumor studies there were no drug-related deaths. Although HCT-116 cells were more sensitive to MLN8054 than PC3 *in vitro*, antitumor activity *in vivo* in these two models were comparable. The discrepancy between *in vitro* and *in vivo* sensitivity is not surprising given the numerous differences between the two systems that can influence growth inhibition, including angiogenesis.

**MLN8054 Treatment Results in Inhibition of Aurora A, Accumulation of Mitotic Cells, and Apoptosis *in Vivo*.** As shown above, treatment of cultured tumor cells with MLN8054 resulted in Aurora A inhibition, mitotic accumulation, and apoptosis. Active Aurora A and mitotic index were measured in mice bearing HCT-116 tumors to confirm the mechanism of action of MLN8054 *in vivo*. Mice received the maximally efficacious dose (a single, 30 mg/kg oral dose). Tumors were removed at various time points over a 24-h period and immunostained for pT288 (active Aurora A) and pHisH3 (mitotic cells).

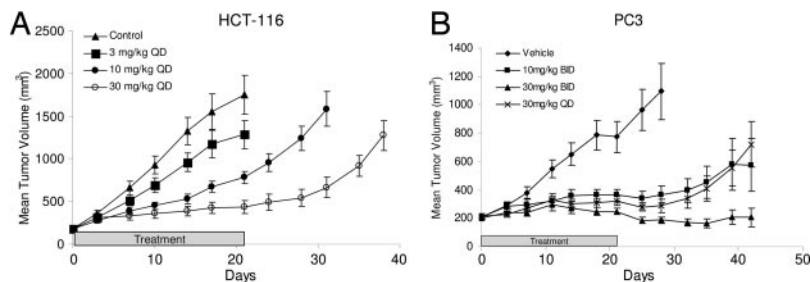


**Fig. 4.** MLN8054 induces TGI in the HCT-116 colorectal and PC3 prostate tumor xenografts. (A) Nude mice bearing HCT-116 tumors were treated orally QD for 21 consecutive days with either vehicle control (▲) or MLN8054 at doses of 3 (■), 10 (●), or 30 (○) mg/kg. Mean tumor volumes (mm<sup>3</sup>)  $\pm$  SEM ( $n = 8$ –10/group) are shown from the initiation of treatment ( $\approx 200$  mm<sup>3</sup>). (B) Nude mice bearing PC3 tumors were treated orally for 21 consecutive days with vehicle control BID (◆) or MLN8054 at 10 mg/kg BID (■), 30 mg/kg BID (▲), or 30 mg/kg QD (×). Mean tumor volumes (mm<sup>3</sup>)  $\pm$  SEM ( $n = 8$ –10/group) are shown from the beginning of treatment.

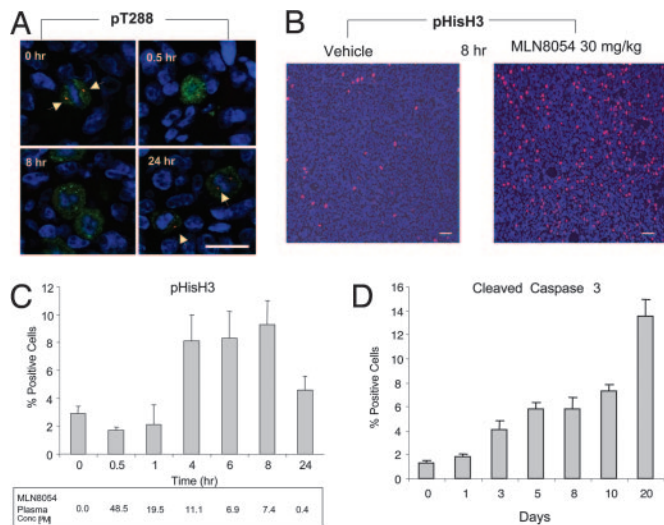


**Fig. 5.** MLN8054 results in inhibition of Aurora A and accumulation of mitotic cells after a single dose and apoptosis after repeat dosing in HCT-116 human tumor xenografts. (A–C) HCT-116 tumor-bearing nude mice were treated orally with a single 30 mg/kg dose of MLN8054, and tumors were removed at various time points for sectioning and immunostaining. DNA (blue) was stained with DAPI to detect all cells in each imaged field. (A) Autophosphorylation of Aurora A on Thr-288 (red, arrows) was determined within mitotic cells (pHisH3-positive; green). (Scale bars, 20  $\mu\text{m}$ .) (B) Mitotic cells (red) were detected by pHisH3 immunostaining and fluorescent microscopy. Shown are representative fields in vehicle-treated control and MLN8054-treated tumors taken 8 h after dosing. (Scale bars, 50  $\mu\text{m}$ .) (C) The percentage of mitotic cells was evaluated at multiple time points throughout a 24-h period. MLN8054 plasma concentrations at each time point were quantified as described in *Methods*. (D) HCT-116 tumor-bearing mice were treated orally with 30 mg/kg MLN8054 BID for 20 consecutive days. Apoptosis was measured by immunofluorescent staining of cleaved caspase 3. (C and D) The percentage of mitotic and apoptotic cells was calculated ( $\pm$  SD) by using automated imaging microscopy ( $n = 3$  mice per time point, 5 images per slide, and 2 slides per tumor) and by dividing the number of mitotic or apoptotic cells by the total number of cells (DAPI-positive).

MLN8054 treatment resulted in a decrease in pT288 staining in the HCT-116 tumor tissue as early as 30 min after administration (Fig. 5A). Inhibition was sustained for  $>8$  h after treatment with signal partially returning by 24 h. There was also a time-dependent increase in mitotic index from a period of 0 to 8 h after treatment ( $\approx 2.5$ - to 3-fold greater than controls) (Fig. 5B) and was declining by the 24-h time point (1.5-fold greater than controls) (Fig. 5C). The plasma concentration of MLN8054 at 8 h was 7.4  $\mu\text{M}$  (Fig. 5C), when effective mitotic arrest occurred. By 24 h, postdosing plasma concentrations had declined to 400 nM, with a corresponding decline in the mitotic index, presumably because concentrations of MLN8054 had fallen below the levels required to inhibit Aurora A. Therefore, a single dose of MLN8054 at 30 mg/kg results in an inhibition of Aurora A and mitotic arrest for a duration between 8–24 h, which is sufficient to induce significant TGI after repeat dosing in this tumor model. The increase in pHisH3-positive (mitotic) cells *in vivo* also is consistent with results seen in cultured cells treated with 0.25–2  $\mu\text{M}$  MLN8054. As previously demonstrated by Aurora kinase inhibitors, a decrease in pHisH3 compared with controls *in vivo* indicates Aurora B inhibition (21, 26). Together, these data suggest that, at the most efficacious dose *in vivo*, MLN8054 treatment results in a phenotype consistent with Aurora A inhibition.

The extent of apoptosis was determined in the HCT-116 tumors grown in mice at various time points throughout a 20-day period of dosing at 30 mg/kg BID. Apoptosis was detected by staining for cleaved caspase 3. A significant increase in the percentage of apoptotic cells compared with day 0 controls was seen after 3 days

of dosing and increased throughout the 20-day period (Fig. 5D). The greatest level of apoptosis was seen after 20 days of dosing with an  $\approx 10$ -fold increase over day 0 controls.

## Discussion

Since its initial identification, Aurora A kinase has been of interest as a potential therapeutic target in oncology. Here, we describe MLN8054, a small-molecule inhibitor that exerts its antitumor activity against human tumor xenografts through inhibition of Aurora A kinase. We specifically demonstrate that MLN8054 treatment of tumor cells results in inhibition of the activating pT288, spindle defects,  $G_2/M$  accumulation, and cell death through apoptosis. These results are consistent with known Aurora A inhibition phenotypes resulting from reduction of protein using RNAi. MLN8054 also demonstrates selectivity for inhibition of Aurora A over the closely related kinase, Aurora B, in tumor cultured cells and xenografts. MLN8054 possesses broad antitumor activity, inhibiting the *in vitro* proliferation of a number of cultured human tumor cell lines and inhibiting the growth of human colon and prostate cancer xenografts after oral administration at well tolerated doses.

Several small-molecule inhibitors of Aurora kinases have been described in the literature (15, 18, 21, 22). Although most of these compounds inhibit Aurora A and Aurora B in enzyme assays, all potently inhibit pHisH3 on Ser-10 and exhibit phenotypes consistent with Aurora B inhibition in cell assays. VX-680 is one such compound currently being evaluated in the clinic (21). Preclinically, this agent demonstrated the ability to inhibit tumor growth *in vivo* but in association with decreases in the pHisH3 signal. Therefore, these compounds are considered to be dual or Aurora B inhibitors. In contrast to these agents, MLN8054 treatment resulted in a decrease in Aurora A autophosphorylation on Thr-288 and an increase in mitotic cells (pHisH3) *in vivo*, results consistent with those seen in cell culture. Aurora A inhibition is seen at doses that induced apoptosis with repeat administration and significantly inhibited tumor growth in colon and prostate cancer models.

It is unknown whether Aurora A or Aurora B is the better target for oncology therapy. In fact, the validity for targeting Aurora A as an anticancer therapeutic approach has been questioned (25) in large part because the major phenotype with pan-Aurora kinase small molecules is consistent with Aurora B inhibition. However, a recent more detailed study demonstrated that pan-Aurora inhibitors also elicit mitotic spindle defects, a phenotype consistent with Aurora A inhibition (24, 27). Our findings with MLN8054 extend the work of others by demonstrating that Aurora A kinase activity is necessary for proper mitotic progression. Moreover, Aurora A inhibition using MLN8054 results in a potent antitumor response in experimental human cancers at well tolerated doses. Clinical studies are underway to evaluate the potential of MLN8054 as an anticancer drug.

## Methods

**Enzyme Assays.** Recombinant murine Aurora A and Aurora B protein were expressed in Sf9 cells and purified with GST affinity chromatography. The peptide substrate for Aurora A was conjugated with biotin (Biotin-GLRRASLG). Aurora A kinase (5 nM) was assayed in 50 mM Hepes (pH 7.5)/10 mM  $\text{MgCl}_2$ /5 mM DTT/0.05% Tween 20/2  $\mu\text{M}$  peptide substrate/3.3  $\mu\text{Ci/ml}$  [ $\gamma$ - $^{33}\text{P}$ ]ATP at 2  $\mu\text{M}$  by using Image FlashPlates (Perkin-Elmer). Aurora B kinase (2 nM) was assayed with 10  $\mu\text{M}$  biotinylated peptide Biotin-TKQTARKSTGGKAPR in 50 mM Tricine (pH 8.0)/2.5 mM  $\text{MgCl}_2$ /5 mM DTT/10% glycerol/2% BSA/40  $\mu\text{Ci/ml}$  [ $\gamma$ - $^{33}\text{P}$ ]ATP at 250  $\mu\text{M}$ . The conditions for all other *in vitro* kinase assays are available upon request. MLN8054 was run in a 226 kinase screen at a 1  $\mu\text{M}$  compound concentration with an ATP concentration of 10  $\mu\text{M}$  for all assays (Upstate Cell Signaling Solutions)



**Immunofluorescence in Cultured Cells.** HCT-116 human tumor cell lines were grown on glass coverslips with MLN8054 diluted in DMSO. Cells treated with DMSO (0.2%) served as the vehicle control. For immunofluorescent staining, the cells were stained with various combinations of anti-Aurora A pT288 rabbit antibody (1:60), anti-IAK/Aurora A kinase mouse monoclonal antibody (1:100), anti-phospho-Ser/Thr-Pro, MPM2 mouse antibody (1:750; Upstate Biotechnology), pHisH3 (Ser-10) mouse monoclonal antibody (1:120), phospho-PLK (Ser-137) rabbit antibody (1:120; Cell Signaling Technology), or anti- $\alpha$ -tubulin mouse antibody (1:1,000; Sigma). Appropriate Alexa Fluor 594 and 488 secondary antibodies were used. Hoescht (1:50,000; Molecular Probes) was used to highlight DNA. Fluorescently labeled cells were visualized with a Nikon TE 300 fluorescent microscope, and images were captured with a digital camera (Hamamatsu). The percentage of mitotic cells was determined by imaging cells with a Discovery-1 High Content Imaging System (Universal Imaging) and by calculating the percentage of Hoescht-stained cells that were positive for MPM2 using Metamorph software (Universal Imaging).

**Aurora A and Aurora B Cell-Based Assays.** HeLa cells were grown on 96-well cell culture dishes for 1 h and 15 min with MLN8054 diluted in DMSO in 2-fold serial dilutions. MLN8054 at each dilution was added as replicates in three to four rows on the dish. Cells treated with DMSO ( $n = 12$ –16 wells per plate; 0.2% final concentration) served as the vehicle control. For the Aurora A assay, cells were stained with phospho-Aurora 2/AIK (T288) rabbit antibody (1:60) and anti-phospho-Ser/Thr-Pro, MPM2 mouse antibody (1:750) followed by Alexa Fluor 488-conjugated goat anti-rabbit IgG (1:180) and Alexa Fluor 594-conjugated chicken anti-mouse IgG (1:180; Molecular Probes). The cells were then stained with Alexa Fluor 488-conjugated chicken anti-goat IgG (1:180; Molecular Probes) and Hoescht (1:50,000). For the Aurora B assay, cells were stained with pHisH3 (Ser-10) monoclonal mouse antibody (1:120) and phospho-PLK (Ser-137) rabbit antibody (1:120) followed by Alexa Fluor 488-conjugated goat anti-rabbit IgG (1:180) and Alexa Fluor 594-conjugated goat anti-mouse IgG (1:180). The cells were then stained with Hoescht (1:50,000).

For cell-based assays, immunofluorescent cells were visualized by using a Discovery-1 High Content Imaging System. Images from 9 or 16 sites per well were captured at  $\times 200$  magnification. For the Aurora A assay, inhibition of Aurora A was determined by measuring pT288 (Aurora A autophosphorylation) fluorescent intensity within MPM2-immunopositive (mitotic) cells by using Metamorph software. Concentration–response curves were generated by calculating the decrease of pT288 fluorescent intensity in MLN8054-treated samples relative to the DMSO-treated controls,

and growth inhibition ( $IC_{50}$ ) values were determined from those curves. For the Aurora B assay, inhibition of Aurora B was determined by counting the number of pPLK137-immunopositive (mitotic) cells that stained positive for pHisH3 by using Metamorph software. Concentration–response curves were generated as described above.

**In Vivo Efficacy Studies.** Female (HCT-116) and male (PC3) athymic nude NCR (*nu/nu*) mice purchased from Charles River Laboratories were used in all *in vivo* studies. Animals had access to food and water ad libitum. All animals were housed and handled in accordance with the Guide for the Care and Use of Laboratory Animals and Millennium Institutional Animal Care and Use Committee guidelines. Eight-week-old nude mice were inoculated with either HCT-116 ( $1 \times 10^6$ ) or PC-3 ( $2 \times 10^6$ ) cells s.c. in the right flank. MLN8054 formulated in 10% hydroxypropyl- $\beta$ -cyclodextrin (Sigma) with 5% sodium bicarbonate was administered orally (100  $\mu$ l). Tumor volumes were measured by using a vernier caliper and calculated with the formula  $L \times W^2 \times 0.5$ . TGI was calculated with the formula  $(\Delta \text{ control average volume} - \Delta \text{ treated average volume}) \times 100 / (\Delta \text{ control average volume})$ .

**In Vivo Mechanism of Action Studies.** Aurora A activity, mitotic index, and apoptosis were measured in frozen tissue sections of control and MLN8054-treated HCT-116 tumors by using immunofluorescent staining for pT288 (rabbit monoclonal generated in-house), pHisH3 (Ser-10) (Cell Signaling Technologies) and cleaved caspase 3 (Cell Signaling Technologies), respectively. Briefly, frozen sections were fixed with fresh 4% paraformaldehyde, and dual immunofluorescent staining was performed to measure Aurora A activity using the pT288 antibody (4  $\mu$ g/ml final concentration) and pHisH3 (1.28  $\mu$ g/ml final concentration). The expression of pT288 was detected by using Rhodamine red-X-conjugated goat anti-rabbit IgG (Jackson ImmunoResearch); pHisH3 was detected by using Alexa Fluor 488-conjugated streptavidin (Molecular Probes). Cells expressing pT288, pHisH3, and/or caspase-3 were detected and imaged by using fluorescence microscopy and quantified with Image Pro Plus software (Media Cybernetics).

**SI.** For further information regarding cell viability, RNAi, Western blot analysis, DNA cell cycle profiling, MLN8054 plasma levels, and statistical analysis, see *SI Methods*.

We thank Mark Rolfe, Mike Cooper, Peter Worland, and Mike Patane for scientific input and the Aurora Drug Safety and Distribution, Protein Sciences, Chemistry, and Biology groups for their contributions.

- Bischoff JR, Anderson L, Zhu Y, Mossie K, Ng L, Souza B, Schryver B, Flanagan P, Clairvoyant F, Ginther C, et al. (1998) *EMBO J* 17:3052–3065.
- Nigg EA (2001) *Nat Rev Mol Cell Biol* 2:21–32.
- Crosio C, Fimia GM, Loury R, Kimura M, Okano Y, Zhou H, Sen S, Allis CD, Sassone-Corsi P (2002) *Mol Cell Biol* 22:874–885.
- Meraldi P, Honda R, Nigg EA (2004) *Curr Opin Genet Dev* 14:29–36.
- Glover DM, Leibowitz MH, McLean DA, Parry H (1995) *Cell* 81:95–105.
- Giet R, McLean D, Descamps S, Lee MJ, Raff JW, Prigent C, Glover DM (2002) *J Cell Biol* 156:437–451.
- Roghi C, Giet R, Uzbekov R, Morin N, Chartrain I, Le Guellec R, Couturier A, Doree M, Philippe M, Prigent C (1998) *J Cell Sci* 111:557–572.
- Hannak E, Kirkham M, Hyman AA, Oegema K (2001) *J Cell Biol* 155:1109–1116.
- Marumoto T, Honda S, Hara T, Nitta M, Hirota T, Kohmura E, Saya H (2003) *J Biol Chem* 278:51786–51795.
- Hata T, Furukawa T, Sunamura M, Egawa S, Motoi F, Ohmura N, Marumoto T, Saya H, Horii A (2005) *Cancer Res* 65:2899–2905.
- Hirota T, Kunitoku N, Sasayama T, Marumoto T, Zhang D, Nitta M, Hatakeyama K, Saya H (2003) *J Cell Sci* 114:585–598.
- Marumoto T, Hirota T, Morisaki T, Kunitoku N, Zhang D, Ichikawa Y, Sasayama T, Kunitoku N, Mimori T, Tamaki N, et al. (2002) *Genes Cells* 7:1173–1182.
- Liu Q, Ruderman JV (2006) *Proc Natl Acad Sci USA* 103:5811–5816.
- Carmenta M, Earnshaw WC (2003) *Nat Rev Mol Cell Biol* 4:842–854.
- Hauf S, Cole RW, LaTerra S, Zimmer C, Schnapp G, Walter R, Heckel A, van Meel J, Rieder CL, Peters JM (2003) *J Cell Biol* 161:281–294.
- Honda R, Korner R, Nigg EA (2003) *Mol Biol Cell* 14:3325–3341.
- Murata-Hori M, Wang YL (2002) *Curr Biol* 12:894–899.
- Ditchfield C, Johnson VL, Tighe A, Ellston R, Haworth C, Johnson T, Mortlock A, Keen N, Taylor SS (2003) *J Cell Biol* 161:267–280.
- Marumoto T, Zhang D, Saya H (2005) *Nat Rev Cancer* 5:42–50.
- Zhou H, Kuang J, Zhong L, Kuo WL, Gray JW, Sahin A, Brinkley BR, Sen S (1998) *Nat Genet* 20:189–193.
- Harrington EA, Bebbington D, Moore J, Rasmussen RK, Ajose-Adeogun AO, Nakayama T, Graham JA, Demur C, Hercend T, Diu-Hercend A, et al. (2004) *Nat Med* 10:262–267.
- Fancelli D, Berta D, Bindi S, Cameron A, Cappella P, Carpinelli P, Catana C, Forte B, Giordano P, Giorgini ML, et al. (2005) *J Med Chem* 48:3080–3084.
- Jung FH, Pasquet G, Lambert-van der Brempt C, Lohmann JJ, Warin N, Renaud F, Germain H, De Savi C, Roberts N, Johnson T, et al. (2006) *J Med Chem* 49:955–970.
- Gadea BB, Ruderman JV (2005) *Mol Biol Cell* 16:1305–1318.
- Keen N, Taylor S (2004) *Nat Rev Cancer* 4:927–936.
- Mortlock A, Keen NJ, Jung FH, Heron NM, Foote KM, Wilkinson R, Green S (2005) *Curr Top Med Chem* 5:199–213.
- Girdler F, Gascoigne KE, Evers PA, Hartmuth S, Crafter C, Foote KM, Keen NJ, Taylor SS (2006) *J Cell Sci* 119:3664–3675.
- Littlepage LE, Wu H, Andresson T, Deanehan JK, Amundadottir LT, Ruderman JV (2002) *Proc Natl Acad Sci USA* 99:15440–15445.
- Satinover DL, Leach CA, Stukenberg PT, Brautigan DL (2004) *Proc Natl Acad Sci USA* 101:8625–8630.
- Giet R, Prigent C (2001) *J Cell Sci* 114:2095–2104.
- Goto H, Yasui Y, Nigg EA, Inagaki M (2002) *Genes Cells* 7:11–17.
- Margolis RL, Lohez OD, Andresson PR (2003) *J Cell Biochem* 88:673–683.
- Vogel C, Kienitz A, Hofmann I, Muller R, Bastians H (2004) *Oncogene* 23:6845–6853.
- Yang H, Burke T, Dempsey J, Diaz B, Collins E, Toth J, Beckmann R, Ye X (2005) *FEBS Lett* 579:3385–3391.